

# Anomalous Hall effect in the Dirac electron system with a split term

Shota Suetsugu, Hiroyasu Matsuura, and Masao Ogata

Department of Physics, University of Tokyo, Hongo, Bunkyo-ku, 113-0033 Japan

E-mail: 6363846388@mail.ecc.u-tokyo.ac.jp

**Abstract.** We study an anomalous Hall effect in the massive Dirac electron system with broken time reversal symmetry. Using the model Hamiltonian with the spin-orbit interaction and a split term which breaks time reversal symmetry, we calculate the energy band, the Berry curvature and the intrinsic Hall conductivity in an analytical way. We show that the non-zero Berry curvature appears and thus an intrinsic Hall conductivity occurs. This anomalous Hall effect can be observed in such systems as a ferromagnetic Dirac electron system or a ferromagnet-coated Dirac electron system.

## 1. Introduction

Anomalous Hall effect is a Hall effect in a ferromagnet without magnetic fields. Its mechanism has been controversial issues [1]. The main mechanisms of the anomalous Hall effect are the intrinsic contribution [2] which is related to the conception of Berry phase [3-5], skew scattering and side jump scattering, and a unified theory of the issues has been revealed [6].

It has been known that unusual quantum Hall effect occurs in graphene which has a massless Dirac Hamiltonian [7,8]. This comes from the existence of non-zero Berry phase around the Dirac point. In addition, the quantized anomalous Hall effect occurs in a N-layer ABC-stacked graphene system with a term which breaks time-reversal symmetry [9]. Moreover, a valley Hall effect occurs in graphene with broken inversion symmetry. [10]

On the other hand, the topological insulators have recently been focused because of the interesting properties of these materials [11,12]. The topological insulator has the gapless band on the surface of a bulk insulator. This band has Dirac-like dispersion and helical spin polarized. The quantized anomalous Hall effect also occurs in the magnetic topological insulator, which is topological insulator doped with transition metal elements such as Cr or Fe [13-15].

Although the anomalous Hall effects in the usual dispersion systems have been well studied, those in the linear dispersion systems like Dirac electron system have not been studied yet. Moreover, the quantized anomalous Hall effect in N-layer graphene depends on a pseudospin which has nothing to do with a real spin, and the magnetic topological insulator is massless Dirac electron system. Therefore, we study in this paper the anomalous Hall effect in the massive Dirac electron system with a real spin.

## 2. Method

In this paper, we discuss the anomalous Hall effect in a massive Dirac electron system. Generally, the anomalous Hall effect occurs in the systems whose Hamiltonian contains a spin-orbit



interaction and a split term due to the internal magnetic field [6]. Therefore, in this paper we use the Wolff Hamiltonian [16] with an isotropic approximation. Cohen and Blount proposed such a Hamiltonian as an effective model of the electrons in Bi [17] and later Wolff found that this Hamiltonian can be rewritten as the  $4 \times 4$  Dirac Hamiltonian. This model contains the spin-orbit interaction in an essential way. In order to study the anomalous Hall effect, we add to this Hamiltonian a split term,  $\Delta\sigma_z$ . Therefore, the Hamiltonian becomes

$$H = \begin{pmatrix} m + \Delta\sigma_z & i\gamma\mathbf{k} \cdot \boldsymbol{\sigma} \\ -i\gamma\mathbf{k} \cdot \boldsymbol{\sigma} & -m - \Delta\sigma_z \end{pmatrix} \\ = \begin{pmatrix} m + \Delta & 0 & i\gamma k_z & i\gamma(k_x - ik_y) \\ 0 & m - \Delta & i\gamma(k_x + ik_y) & -i\gamma k_z \\ -i\gamma k_z & -i\gamma(k_x - ik_y) & -m - \Delta & 0 \\ -i\gamma(k_x + ik_y) & i\gamma k_z & 0 & -m + \Delta \end{pmatrix}$$

where  $m$  represents the mass gap and we use typical set of parameters,  $m = 10$  (meV) and  $\gamma = 10^{-7}$  (meV m). Because the sign of a magnetic moment is opposite between conduction and valence bands [18], the split terms have opposite signs. Note that this split term breaks time reversal symmetry.

The intrinsic Hall conductivity of this system is given by

$$\sigma_{xy} = \sum_n \frac{e^2}{\hbar} \int \frac{d\mathbf{k}}{(2\pi)^d} \Omega_{k_x k_y}^n(\mathbf{k}) f(E(\mathbf{k})),$$

where  $f(E(\mathbf{k}))$  is the Fermi distribution function and  $\Omega_{k_x k_y}^n$  given by

$$\Omega_{k_x k_y}^n(\mathbf{k}) = i \left( \left\langle \frac{\partial n(\mathbf{k})}{\partial k_x} \middle| \frac{\partial n(\mathbf{k})}{\partial k_y} \right\rangle - (x \leftrightarrow y) \right)$$

is the Berry curvature of the  $n$ -th band [3]. This formula is derived from Kubo formula. Although the bands in real systems have a cutoff, the  $\mathbf{k}$  integral is taken over all  $\mathbf{k}$  values. When the non-zero Berry curvature exists, the velocity becomes

$$\mathbf{v}_n = \frac{\partial E_n(\mathbf{k})}{\hbar \partial \mathbf{k}} + \frac{e}{\hbar} \mathbf{E} \times \boldsymbol{\Omega}^n(\mathbf{k})$$

where  $\mathbf{E}$  is a electric field. This contribution from the Berry curvature known as an anomalous velocity is related to a Hall current. In the following, we calculate the energy band, the Berry curvature and the intrinsic Hall conductivity at  $T = 0$  by

$$\sigma_{xy} = \sum_n \frac{e^2}{\hbar} \int_{E_n(\mathbf{k}) < E_f} \frac{d\mathbf{k}}{(2\pi)^d} \Omega_{k_x k_y}^n(\mathbf{k})$$

in an analytical way. Here,  $E_f$  is the Fermi energy. Note that the whole Hall conductivity has other contributions such as the extrinsic contribution which comes from impurities.

In the same way as in the three-dimensional case, we also study the two-dimensional case which is obtained by ignoring  $k_z$  dependence. The integration in the Hall conductivity formula is also carried out in the two-dimensional  $\mathbf{k}$ -space.

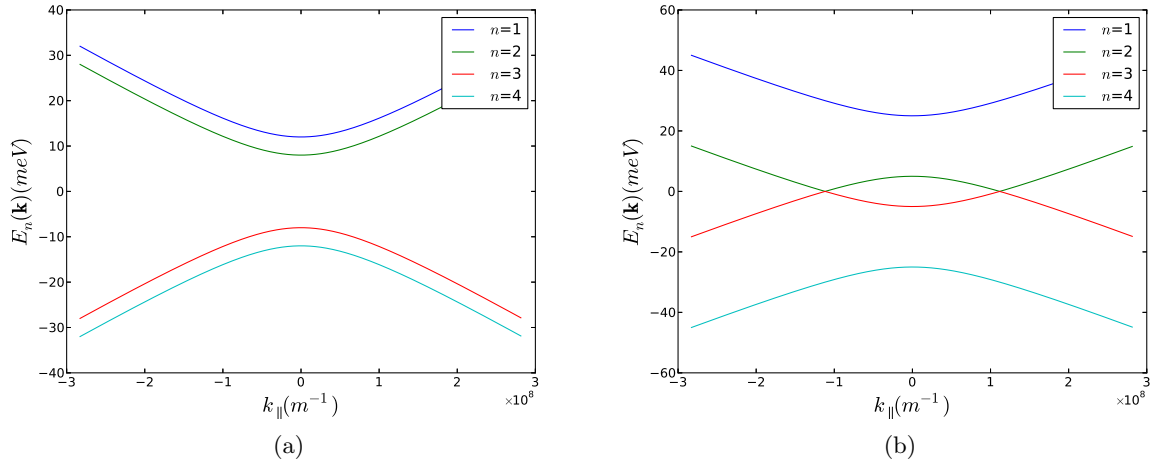


**Figure 1.** Energy Band of this system. Here  $k_{\parallel}^2 = k_x^2 + k_y^2$ . (a)  $m \geq \Delta$  case. ( $\Delta = 2(\text{meV})$ ) (b)  $m \leq \Delta$  case. ( $\Delta = 15(\text{meV})$ ) In this case, the second- and the third-band avoid crossing.

### 3. Result

By diagonalizing the Hamiltonian, we obtain the energy band as

$$E_n = \pm \sqrt{m^2 + \Delta^2 + \gamma^2 k^2 \pm 2\Delta \sqrt{m^2 + \gamma^2(k_x^2 + k_y^2)}} \quad (n = 1, \dots, 4),$$

where  $n$  is the band index in descending order. Figure 1 shows examples of this band dispersion for typical cases.

Using the eigenfunctions, we calculate Berry curvature of this model,

$$\Omega_{k_x k_y}^n = \pm \frac{m\gamma^2}{2(m^2 + \gamma^2(k_x^2 + k_y^2))^{3/2}} \quad (+ : n = 2 \text{ or } 3, - : n = 1 \text{ or } 4)$$

Opposite signs of the Berry curvature mean that the bands  $n = 1$  and  $2$  ( $n = 3$  and  $4$ ) have the opposite signs anomalous velocity. Note that the Berry curvatures vanishes when the bands are not split and the bands  $n = 1$  and  $2$  ( $n = 3$  and  $4$ ) are degenerate. Since the energy bands and the Berry curvatures are symmetric with respect to energy, we consider the cases with  $E_f > 0$  and calculate the first- and the second-band contributions in the following.

Owing to the population difference in the spin-up and spin-down electrons, the intrinsic Hall

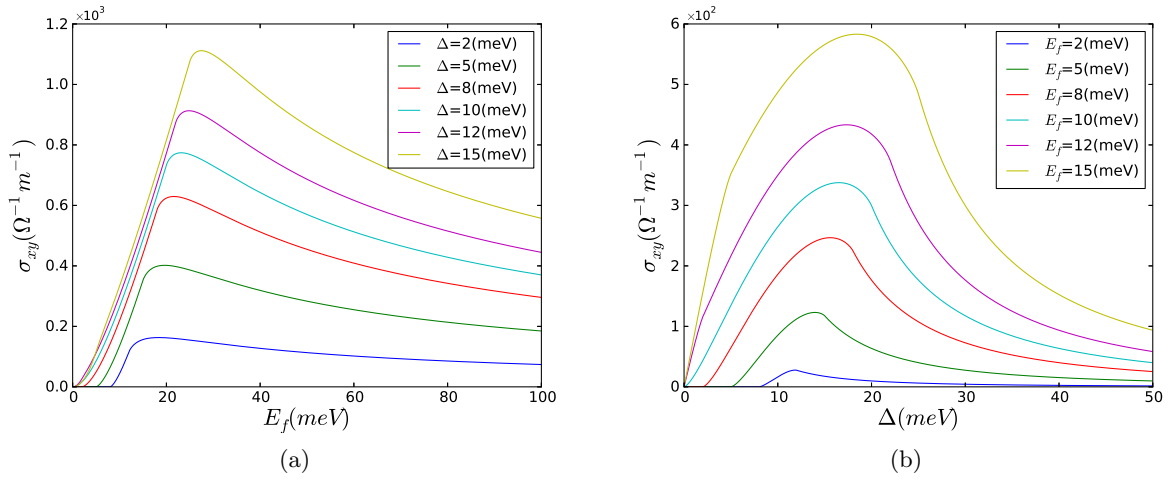


**Figure 2.** The intrinsic Hall conductivity calculated from the Berry curvature. These are the sum of the contribution from the first- and the second-band. (a) The  $E_f$  dependence of the intrinsic Hall conductivity. (b) The  $\Delta$  dependence of intrinsic Hall conductivity.

conductivities for the first- and the second-band occur and these are obtained analytically as

$$\begin{aligned} \frac{\sigma_{xy}^{(1)}}{\frac{e^2}{h}} &= -\frac{E_f}{2\pi\gamma} \sqrt{1 - \left(\frac{m+\Delta}{E_f}\right)^2} + \frac{m}{2\pi\gamma} \arccos\left(\frac{m+\Delta}{E_f}\right) \\ &+ \frac{m}{2\pi\gamma} \frac{\Delta}{\sqrt{E_f^2 - \Delta^2}} \ln \left( \frac{\sqrt{(E_f - \Delta)(E_f + m + \Delta)} + \sqrt{(E_f + \Delta)(E_f - m - \Delta)}}{\sqrt{(E_f - \Delta)(E_f + m + \Delta)} - \sqrt{(E_f + \Delta)(E_f - m - \Delta)}} \right) \\ &\quad (E_f > m + \Delta) \\ \frac{\sigma_{xy}^{(2)}}{\frac{e^2}{h}} &= \frac{E_f}{2\pi\gamma} \sqrt{1 - \left(\frac{m-\Delta}{E_f}\right)^2} - \frac{m}{2\pi\gamma} \arccos\left(\frac{m-\Delta}{E_f}\right) \\ &\quad \left\{ \begin{array}{l} + \frac{m}{2\pi\gamma} \frac{\Delta}{\sqrt{E_f^2 - \Delta^2}} \ln \left( \frac{\sqrt{(E_f + \Delta)(E_f + m - \Delta)} + \sqrt{(E_f - \Delta)(E_f - m + \Delta)}}{\sqrt{(E_f + \Delta)(E_f + m - \Delta)} - \sqrt{(E_f - \Delta)(E_f - m + \Delta)}} \right) \quad (E_f > |m - \Delta|, E_f > \Delta) \\ + \frac{m}{2\pi\gamma} \frac{2\Delta}{\sqrt{\Delta^2 - E_f^2}} \arctan \left( \sqrt{\frac{(\Delta - E_f)(E_f - m + \Delta)}{(E_f + \Delta)(E_f + m - \Delta)}} \right) \quad (|m - \Delta| < E_f < \Delta) \end{array} \right. \\ \frac{\sigma_{xy}^{(2)}}{\frac{e^2}{h}} &= \frac{1}{2\pi} \frac{m\pi}{\gamma} \left( \frac{\Delta}{\sqrt{\Delta^2 - E_f^2}} - 1 \right) \quad (0 \leq E_f \leq \Delta - m) \end{aligned}$$

where  $\sigma_{xy}^{(n)}$  is the contribution from the  $n$ -th band.

There are two reasons why the analytic form of the intrinsic Hall conductivity changes depending on the parameters,  $E_f$ ,  $m$ , and  $\Delta$ . Firstly, since the first band has a band minimum at  $E = m + \Delta$ , it starts to contribute to  $\sigma_{xy}$  when  $E_f$  exceeds  $m + \Delta$ . Secondly, anticrossing of the second band changes the range of integration when  $\Delta > m$ .

Figure 2 (a) shows the intrinsic Hall conductivity as a function of  $E_f$ . It begins to increase at  $E_f = m - \Delta$  and starts to decrease near  $E_f = m + \Delta$ . This is because the second-band which has the positive Berry curvature starts to contribute to  $\sigma_{xy}$  at  $E_f = m - \Delta$  and the first-band which has the negative Berry curvature joins from  $E_f = m + \Delta$ . Figure 2 (b) shows that the intrinsic Hall conductivity is 0 at  $\Delta = 0$  because the bands are not split on this occasion.

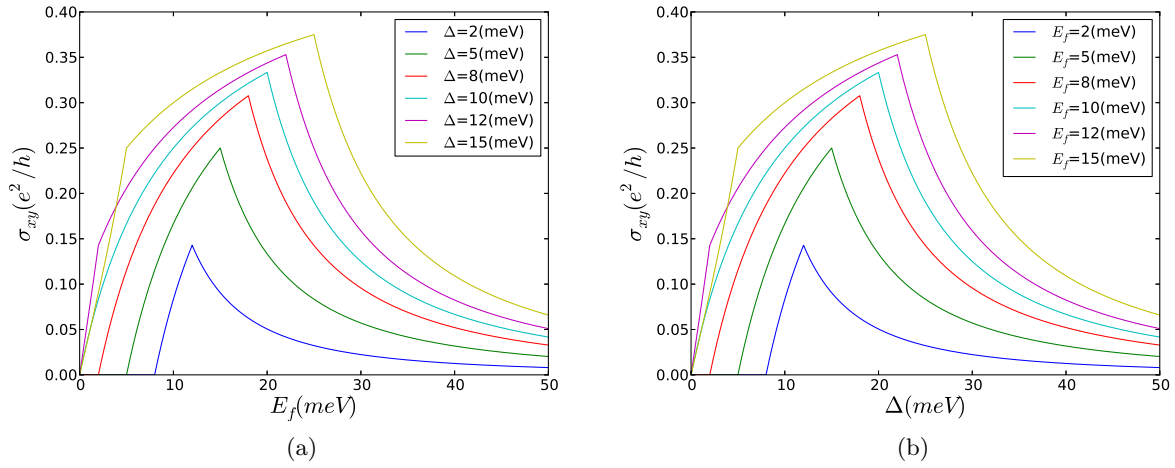


**Figure 3.** The intrinsic Hall conductivity in the two-dimensional case. (a) The  $E_f$  dependence of the intrinsic Hall conductivity. (b) The  $\Delta$  dependence of intrinsic Hall conductivity. However, this is identical with (a).

In the two-dimensional system, the energy bands and the Berry curvatures are obtained by replacing  $k_z$  with 0. The intrinsic Hall conductivity is given by

$$\frac{\sigma_{xy}}{h} = \begin{cases} \frac{1}{2} \frac{E_f + \Delta - m}{E_f + \Delta} & (m - \Delta < E_f < m + \Delta, m > \Delta \quad \text{or} \quad \Delta - m < E_f < \Delta + m, \Delta > m) \\ \frac{m\Delta}{(E_f - \Delta)(E_f + \Delta)} & (m + \Delta < E_f) \\ \frac{mE_f}{(\Delta - E_f)(\Delta + E_f)} & (0 < E_f < \Delta - m, \Delta > m) \end{cases}$$

Interestingly, this formula is symmetric with respect to exchange of  $E_f$  for  $\Delta$ . This is clearly shown in Figure 3.

#### 4. Conclusion

In this paper, we showed that the anomalous Hall conductivity occurs in the massive Dirac electron system with a spin-orbit interaction and a split term. Unlike the magnetic topological insulator, the anomalous Hall conductivity is not quantized. This is because the quantized anomalous Hall effect in the magnetic topological insulator originates from the massless Dirac fermion.

Although we only studied the system with broken time reversal symmetry in this paper, it is interesting to study the systems in which other symmetries are broken. In the  $N$ -layer graphene system, it has been shown that some interesting quantum phases occur [9]. In addition, a valley Hall effect in graphene with broken inversion symmetry [10] is essentially similar to our result in the two-dimensional case except for a kind of broken symmetry. Therefore, it is interesting to study the system with broken inversion symmetry in the three-dimensional case.

Experimentally, this anomalous Hall conductivity will be observed in such systems as a ferromagnetic Dirac electron system or a ferromagnet-coated Dirac electron system. In this paper, only the intrinsic contribution was considered. Other contributions, such as the extrinsic contribution from impurities, will be observed in experiments, so further calculation is necessary for the extrinsic contribution. However, the result of this paper will help to identify the intrinsic contribution by measuring the chemical potential dependence and the split gap dependence.

## References

- [1] N. Nagaosa et al. 2010 *Rev. Mod. Phys.* **82**, 1539
- [2] R. Karplus and J. M. Luttinger 1954 *Phys. Rev.* **95**, 1154
- [3] D. Xiao et al. 2010 *Rev. Mod. Phys.* **82**, 1959
- [4] M. Onoda and N. Nagaosa 2002 *J. Phys. Soc. Jpn.* **71**, 19-22
- [5] T. Jungwirth et al. 2002 *Phys. Rev. Lett.* **88**, 207208
- [6] S. Onoda et al. 2006 *Phys. Rev. Lett.* **97**, 126602
- [7] N. M. R. Peres et al. 2006 *Phys. Rev. B* **73**, 125411
- [8] Y. Zhang et al. 2005 *Nature Phys.* **438**, 201-204
- [9] F. Zhang et al. 2011 *Phys. Rev. Lett.* **106**, 156801
- [10] D. Xiao et al. 2007 *Phys. Rev. Lett.* **99**, 236809
- [11] L. Fu et al. 2007 *Phys. Rev. Lett.* **98**, 106803
- [12] D. Hsieh et al. 2008 *Nature* **452** 970-974
- [13] R. Yu et al. 2010 *Science* **329**, 61
- [14] C. Chang et al. 2013 *Science* **340**, 167
- [15] J. G. Checkelsky et al. 2014 *Nature Phys.* **10**, 731736
- [16] P. Wolff 1964 *J. Phys. Chem. Solids* **25**, 1057
- [17] M. Cohen and E. Blount 1960 *Philos. Mag.* **5**, 115
- [18] Y. Fuseya et al. 2011 *J. Phys. Soc. Jpn.* **81**, 013704